

PHASE 4: Assembly and Prototype Report

Austin Matthew Brown

James Guentert

Kaitlyn Novy

Lauren G. Tidyman

Lv "Elvis" Trexler

Rajvir Singh

Table of Contents

— Existing Research and Object	2 - 4
— Design	4 - 34
A. Assembly and Part SolidWorks Video	4
B. Materials and Prototyping	5 - 8
C. Construction Instructions	8 - 14
D. Cost Analysis and Results	14 - 16
E. Iterative Testing and Results	16 - 34
a. Design Input Insights	
b. Physics Simulations	
c. Results	
d. Engineering Drawings	
— References	35 - 36

Existing Research and Objective

Across the world, minimally invasive procedures such as biopsies, ablations, and targeted drug deliveries are becoming increasingly common due to their shorter recovery times, reduced pain, and lower risk of complications. However, a critical limitation persists in the precision required to guide needles to internal targets using CT imaging. Traditional methods of manual triangulation are prone to error—surgeons often rely on visual estimation to align a needle within the correct angle and imaging “slice,” which can lead to misalignment and failed targeting, especially in deep or small lesions.

In CT-guided biopsies, even slight errors in angling or positioning can cause the needle path to deviate outside the target zone, compromising diagnostic accuracy and increasing patient

risk. In one experiment, researchers found that with wrongful alignment, “a pneumothorax had been created in one patient, and the spleen was inadvertently punctured in

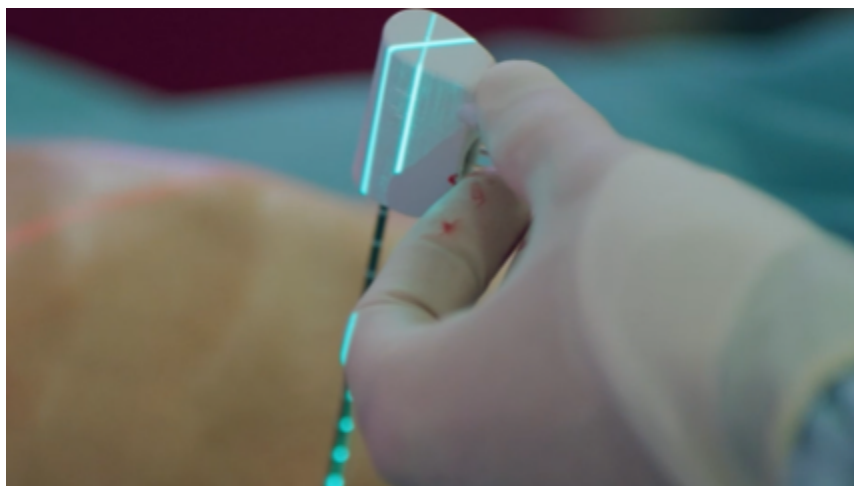


Figure 1: Current CT-guided needle angling technology(Siemens)

of the calculated angled approach, the pleura was not violated in any patient and no other

complications occurred"(E. VanSonnenberg, 3). These limitations are particularly detrimental in under-resourced clinical settings, where access to training, advanced guidance systems, or robotic tools is limited. Without standardization, procedural outcomes heavily depend on practitioner experience, thereby exacerbating healthcare disparities. This is why our group focused on developing a reliable, low-cost, and open-source solution to enhance needle accuracy in image-guided interventions.

Our proposed device—a handheld, ergonomic, angular needle guide—eliminates the need for manual triangulation by providing physical aids to ensure alignment in both angle and imaging slice. With only depth already marked on standard needles, our guide introduces mechanical assistance for the other two spatial dimensions—slice and angle—thus completing the three-dimensional targeting process.

We designed our solution, called the Needle Guider, to be 3D printable, metal-free (to avoid imaging artifacts), intuitive to use, and easily manufacturable. It requires no electronics or specialized training, making it ideal for global application, especially in settings where precision is critical and resources are minimal. A recent clinical study evaluating CT-guided needle insertion techniques highlighted the performance gap between manual and robotic methods. The researchers reported that, "compared to manual insertion without the use of a navigation device, robotic insertion has advantages which include accurate needle targeting before insertion and needle stability during insertion" (Hiraki et al., 5). While robotic systems offer excellent results, their cost and complexity limit accessibility. Our device aims to provide those same targeting

benefits—accuracy and stability—in a low-cost, manual alternative. Our goal is to level the surgical playing field by providing every practitioner—regardless of experience or access—with a tool to safely and accurately guide needles.

Design

A. Assembly and Parts SolidWorks Video

Video Link: <https://www.youtube.com/watch?v=onuLIYW7PKY>

Video Chapters:

[Base Plate Build Tutorial](#)

[Sliding Track Build Tutorial](#)

[Sliding Track Build Tutorial](#)

[Slider Attachment Build Tutorial](#)

[Syringe Clip Build Tutorial](#)

[Assembly Tutorial](#)

[Simulations](#)

B. Materials and Prototyping

The needle guide must be constructed from materials that exhibit stiffness, water resistance, heat resistance, recyclability, biocompatibility, and the ability to withstand

sterilization processes. As a Class I medical device, it is imperative that the needle guide is fabricated from medical-grade materials that comply with ISO 10993 standards, as verified by the FDA (“Product Classification,” 2025). The needle guide makes direct contact with the patient’s skin through the silicone base. In the medical field, “silicones are used because of their biocompatibility in a wide variety of physical forms,” and are noted for their “biocompatibility in a wide variety of physical forms” (X. Thomas, 1). For the needle guide silicon support, the silicone material must possess a duality of flexibility and rigidity. It should conform to the contours of the

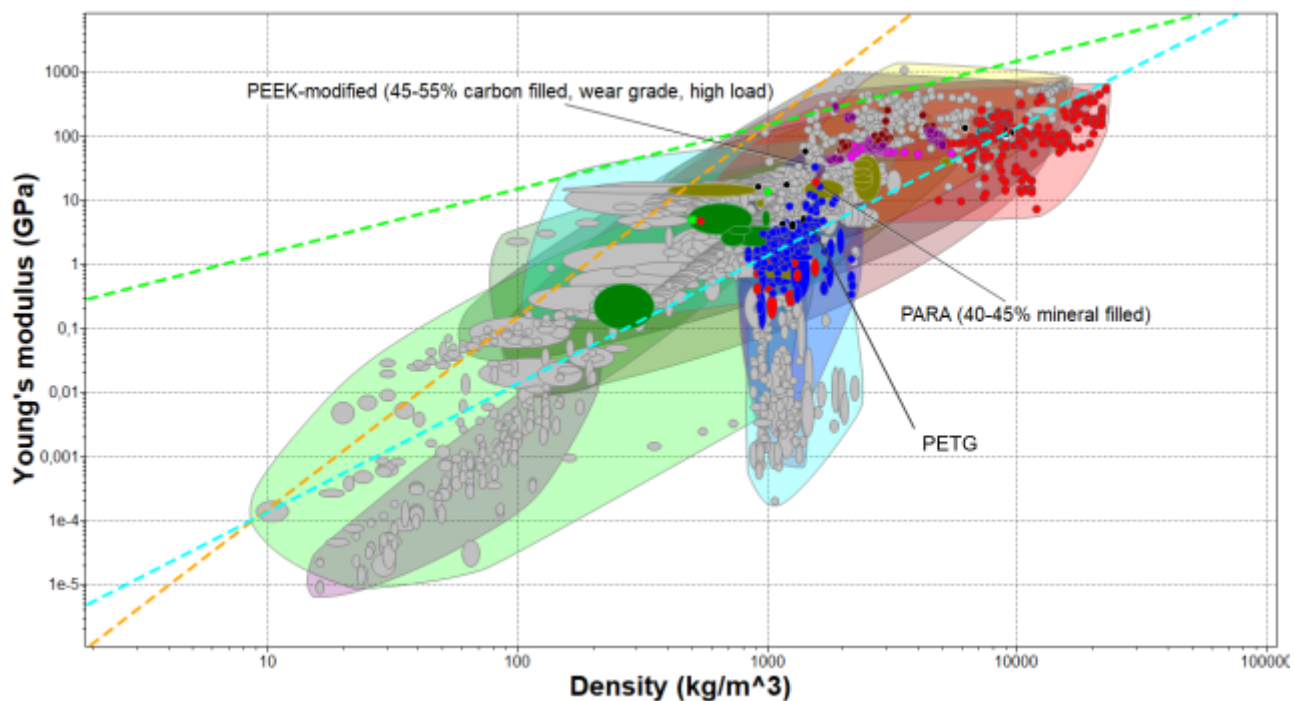


Figure 1 | Ashby Chart. The figure is of an Ashby chart with the limits on the minimum Young's modulus (above or equal to 0.28 GPa) and recyclability. The dark blue region is plastics and the light blue region is elastomers. The neon green line corresponds to E/p , the aqua blue line corresponds to $E^{(1/2)}/p$, and the orange lines corresponds to $E^{(1/3)}/p$.

patient's anatomy while ensuring that the needle guide achieves a flat orientation within the base.

Furthermore, the silicone must exhibit water and heat resistance. The optimal choice for the

Properties	Categories			
	PEEK	PTFE	PPO	PI
Tensile strength/MPa	97.4	20.3	66.5	116.2
Tensile modulus/GPa	2.8	0.4	2.7	
Flexural strength/MPa	142.1	12.9	109.7	176.2
Flexural modulus/GPa	3.7		2.0	3.3
Compression strength/MPa	130	12	100	148
Charpy Notched Impact Strength / kJ·m ⁻²	4.44	0.16	0.09	0.10
Linear expansion coefficient/10 ⁻⁵ K ⁻¹ (10-180°C)	4.8	11	5.6	4.8
Thermal distortion temperature /°C(1.82MPa)	152	55	190	

Figure 2 | Table of Temperature Resistant Plastics. A table of properties of popular plastics from the study “Polyether Ether Ketone (PEEK) Properties and Its Application Status.”

silicon support is Polydimethylsiloxane (PDMS). PDMS is characterized by its optical clarity, chemical inertness, and non-toxicity. It is non-flammable and offers excellent flexibility and stretchability, alongside low surface tension and good thermal stability.

Additionally, PDMS demonstrates notable

biocompatibility, corrosion resistance, pliability,

chemical inertness, homogeneity, and minimal water absorption, making it well-suited for medical applications. PDMS “polymers do not require stabilizers because of their intrinsic stability” and also “do not require plasticizers because of their low Tg” (X. Thomas, 1). Hence, PDMS is the best choice of silicone for the silicone support of the needle guide.

When selecting the material for the 3D-printed components, the 90-degree arc serves as the reference. Initial testing establishes that the average force exerted on the arc is approximately 1 N. Notably, the highest recorded force for a 1 mL syringe, using a 26G needle, is 1.15 N, while the lowest force, observed with a 27G spinal needle, is 0.75 N (Prasetyono et al., 2019). To account for variability, we take a generous estimate and assume an average force of 2 N acting on the arc. Additionally, we define a tolerable extension length of 0.08 mm. Based on these parameters, we proceed to calculate the strain, stress, and Young's modulus of the arc:

$$\text{Strain: } \epsilon = \delta l / l_0 = 0.08 \times 10^{-3} m / 0.1296 m \approx 6.173 \times 10^{-3}$$

$$\text{Stress: } \sigma = F/A_c = 2N / 0.0001125 m^2 \simeq 17777.78 Pa$$

$$\text{Young's Modulus: } \sigma/\epsilon = 17.78 Pa / 6.173 \times 10^{-3} = 28800000 Pa = 2.8 \times 10^{-1} GPa$$

The 90-degree arc is assumed to be a “beam” with maximum stiffness governed by the equation

$E^{1/2}/\rho$. In Figure 1, three materials stand out: (1) PEEK-modified(45-55% carbon filled, wear grade, high load, (2) PARA (40-45% mineral filled), and (3) PETG. PEEK is a semicrystalline thermoplastic with a Young's modulus of 3.6 GPa, and its tensile strength is 90 to 100 MPa. PARA (Polyaramide) is characterized by its resistance to thermal and water degradation (Ling, Xuanzhe, et al., 2020). As a semicrystalline polymer, it is commonly reinforced with fiber or mineral fillers. PARA exhibits superior chemical resistance and demonstrates a lower moisture absorption rate compared to its polyamide counterpart, PA. Its rigidity is maintained across a temperature range of 25°F to 280°F. PETG, or Polyethylene Terephthalate Glycol-modified, is a thermoplastic copolymer that exhibits superior thermal stability and moisture resistance, coupled with robust tensile strength and durability. Similar to its polyester counterpart, PET, PETG is fully recyclable, making it a sustainable option in various applications. Its favorable processing characteristics and high clarity make it particularly advantageous for fabricated products requiring both resilience and aesthetic appeal.

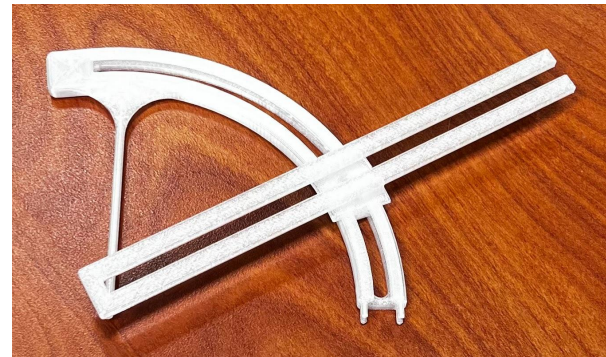
Both PEEK and PARA exhibit remarkable durability, but PETG has been identified as the most suitable material for the needle guide. Its enhanced water resistance, superior durability, and positive sustainability attributes make PETG the preferred choice. Notably, while PETG is the

densest of the three materials, it remains relatively lightweight. This characteristic contributes to improved maneuverability, greater patient comfort, and more convenient transport. Hence, the material selected for the 3D printed needle guide components is PETG.

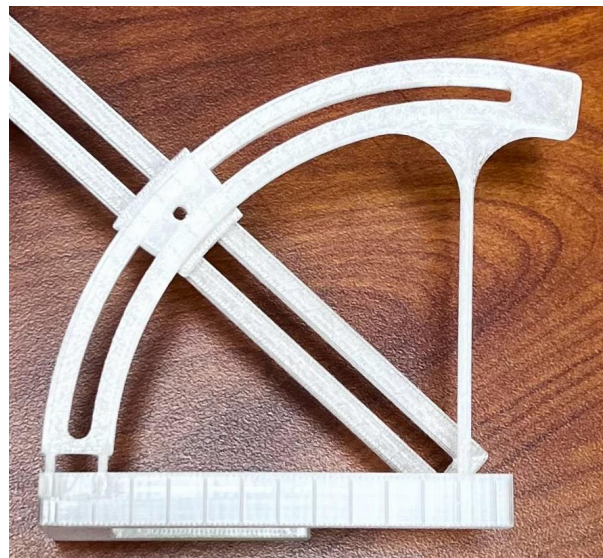
C. Construction Instructions

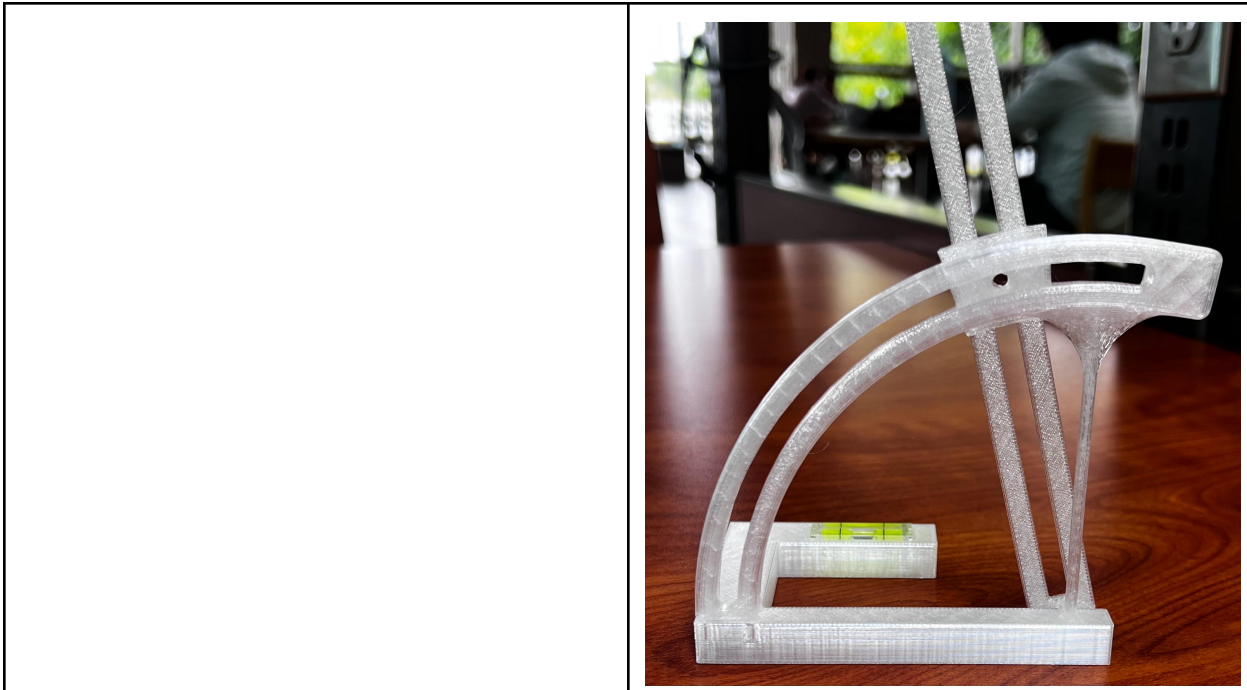
<p><i>STEP 0:</i> 3D print all pieces of the product, remove from the magnetic plate</p>	
<p><i>STEP 1:</i> Remove all supports from 3D printed parts. Sand and deburr all rough edges to remove leftover supports</p>	

STEP 2: Thread the sliding track rotator into the rotator track



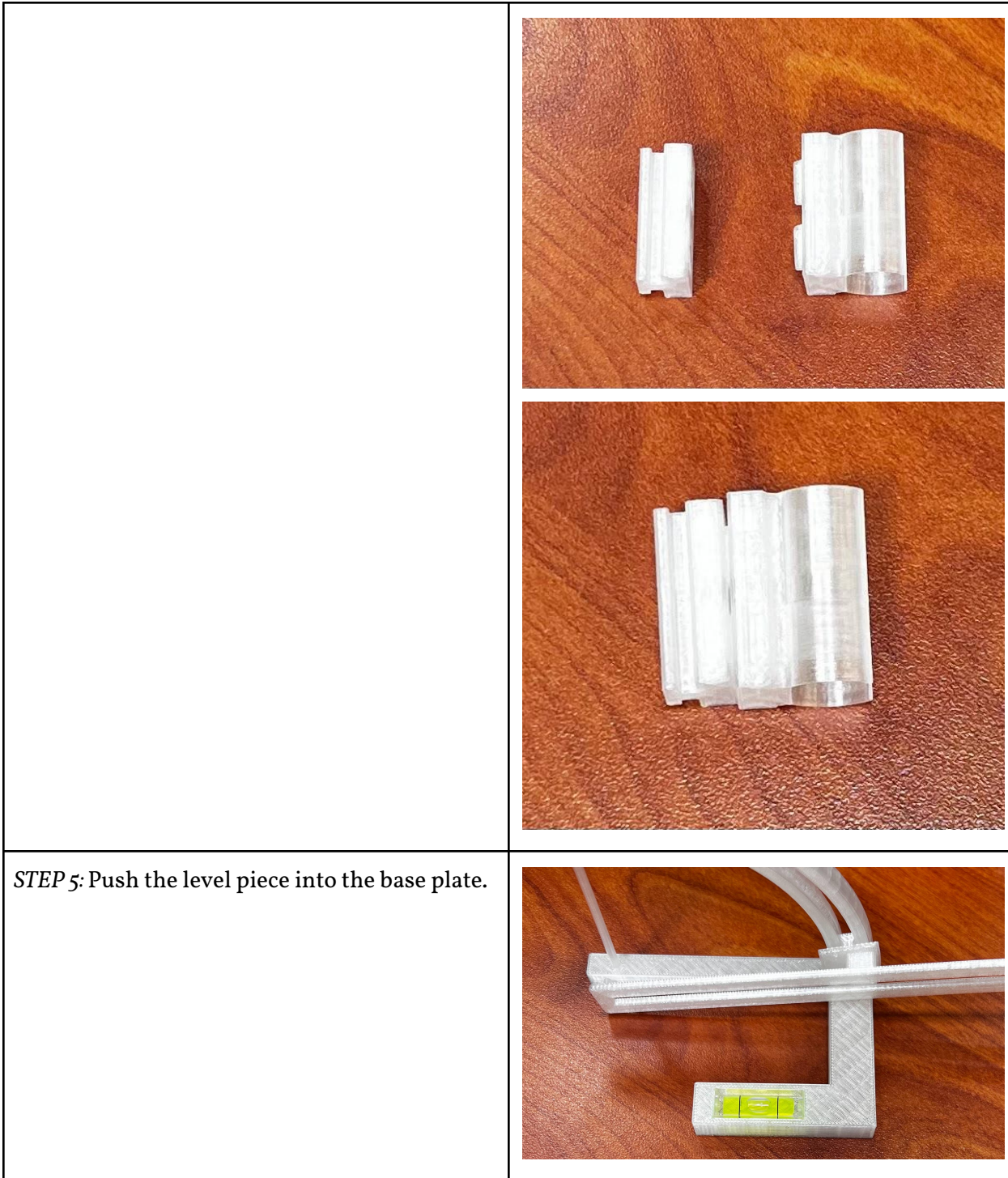
STEP 3: Connect the rotator track to the base plate by sliding the pins of the rotator track into the pin holes on the base plate.



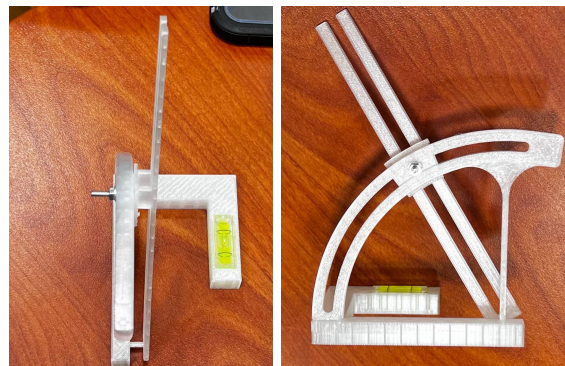


STEP 4: Assemble the syringe clip and slide attachment by aligning the two pieces and clicking them together.

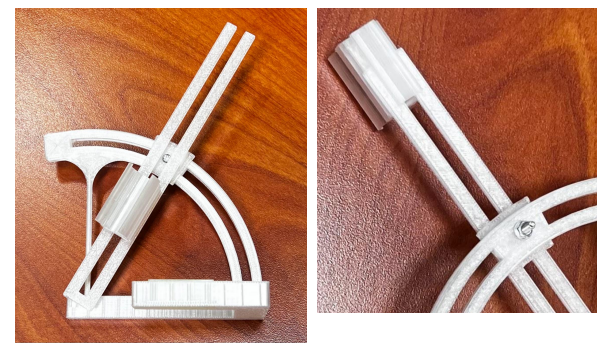




STEP 6: Thread the M-3 screw through the sliding track rotator and the rotator track, and secure it in place by using a washer and nut on the back side of the rotator track.



STEP 7: Slide the slider attachment, fixed to the syringe clip, onto the sliding track rotator.



STEP 8: Attach the syringe to the syringe clip.



D. Cost Analysis and Results

Quantity	Item	Cost
I	550 Pcs Screws Bolts and Nuts Assortment Kit, Metric Machine Screws and Nuts and Flat Washers, M3/M4/M5 Slotted Pan Head Hex Bolts Sets (B)	\$12.98
I	Silicone Sponge Human Skin Injection Pad Training Model, Nurse Student Practice, No Syringe Included!!!	\$8.99
I	20 Pack Plastic Syringe Luer Lock with Needle - 10ml, 5ml, 3ml, 1ml Syringes and 18Ga, 22Ga, 23Ga, 25 Ga Needle, Individually Sealed Package	\$9.99
I	1InTheOffice Protractor Geometry, Clear Protractor, Plastic Protractor 6 Inch, 180 Degrees, 6 Pieces	\$8.29
I	11pcs Mini Level Picture Hanging Spirit Bubble Level, 10x10x29mm Square Level Mark Measuring Tools	\$4.99
I	LET'S RESIN Silicone Putty, 1LB/40A Mold Making Kit, Non-Toxic, Strong & Flexible, Easy 1:1 Mixing Ratio for Reusable Silicone Molds, Resin, Soap	\$22.46
I	Dianrui 300PCS Compression Springs Assortment Kit 23 Different Sizes Mini Spring Stainless Steel Mechanical Small Springs for DIY Repair Project	\$8.99

I	E-outstanding 600pcs M1 M1.2 M1.4 M2.5 Mini Electronics Screws Nuts Assortment Tool Kit 12 Kinds of Repair Hardware Tools Box with Screwdriver for Electronic Products	\$9.59
I	First 3D Print Order	\$24
I	Second 3D Print Order	\$12
I	Third 3D Print Order	\$12
Total:		<u>\$134.28</u>

The screw, washer, and nut assortment kit were used to secure the sliding track rotator piece to the rotator track, allowing for the sliding track rotator to lock in place while the needle is inserted. The silicone skin pad was purchased for demonstrations of needle insertion at specific angles, as well as to ensure the device worked as intended. Syringes were purchased at varying sizes to use in demonstrations of the needle guide, ensuring the needle guide could accommodate the size and shape of the syringe barrel and needle, finally the syringes were also used in determining sizing for the syringe clip (piece that holds the syringe on needle guide), allowing multiple clip sizes to be created accommodating different size syringe barrels. The protractor was used to evaluate the angle measurements on our device, to ensure the angles lined up as planned. Levels were inserted into the device to ensure it was perfectly aligned and leveled, if needed. Silicone putty was purchased for the idea of possible removable silicone pads placed on the underside of the base, which would attach to the device and allow for greater conformity to the

patient. Compression springs were intended for earlier renditions of the device and were eventually phased out of the final design. The mini electronic screws, washers, and nuts were purchased for earlier renditions of the device and were phased out of the final design in favor of the M-3 screw, washer, and nut. Three designs were printed. The first print revealed that our scale was incorrect and required our design to be significantly reduced in size. The second print was perfect until we discovered minor sizing errors that needed correction. The third print incorporated all corrections and became our final product. Our final costs were comfortably within our \$215 budget due to several factors, including the miniature size and the limited number of components. Off-the-shelf components: used purchased items total: \$67.70, unused purchased items total: \$18.58, and combined final total: \$86.28. The total cost of 3D printing was approximately \$48. All together, our project's combined total came to \$134.28.

E. Iterative Testing and Results

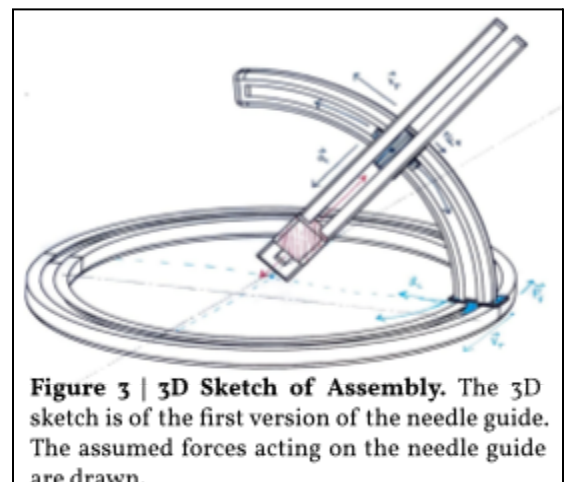
a. Design Input Insights

Interacting with this challenge revealed that inaccuracy in syringe placement stems from excessive freedom of movement and that an effective solution must begin by eliminating unnecessary degrees of freedom during operation. To constrain movement, we modeled the syringe such that its tip is treated as a point in 3D space, with a defined insertion vector representing the needle's orientation and linear path. This immediately ruled out systems that were purely rotational or purely translational, as both types of motion are required for precise

needle guidance. We also recognized that any coordinate system with more than three adjustable parameters introduced redundancy. For example, our early “tower” design utilized height, dual-axis rotation, and a sliding track—but these controls overlapped, allowing multiple distinct setups to yield the same final needle trajectory. Since tilt, slice, and depth are the only clinically relevant parameters provided preoperatively, the device should control only those three, and do so independently. This insight led us to structure the device around a spherical coordinate-inspired model. Specifically, this model is restricted to a half sphere, which prevents all motion except tilt, slice, and depth. Parameters can then be assigned to these three factors, such as keeping the slice constant, as the location of the base plate remains the same once the device's location is chosen. Tilt can vary between 7.5 and 90 degrees at any instance, and varying lengths of needles can be chosen from the operation table. This configuration aligns closely with clinical workflow while minimizing ambiguity and user error.

First Iteration Design

Our first iteration of the spherical-coordinate-inspired design featured a circular base composed of two interlocking 180-degree arc rails, forming a full ring. A rotating carriage traversed this base, acting as the azimuthal adjustment for slice orientation. Mounted to this carriage was a pivoted vertical arc segment (spanning 97



degrees) that functioned as a polar angle guide. This arc housed a rotating platform or gimbal joint that adjusted the tilt of an attached linear rail system, along which the syringe carriage translated to control insertion depth. The pivot points and sliding interfaces were implemented using clearance fits and axial pins. This design revealed several key areas for improvement. First, the circular base occupied excessive horizontal space, which posed a significant issue—the accuracy of angular and slice measurements depended on the assembly remaining level with the ground. A larger footprint made stable positioning more difficult, especially in constrained clinical environments. Additionally, the unsupported vertical arc introduced structural weaknesses. Without a central support or brace, the arc was subjected to torque-induced stress from the cantilevered syringe load, particularly at steeper angles of inclination. This can lead to deformation of the base tracks and jittery movement, with the severity of deflection varying based on the configuration and weight distribution of the syringe.

Key Changes Made

The original circular base design proved far too bulky for clinical use. Its large footprint often prevented the device from sitting flush on the patient's skin, and it was not ergonomically suited for handheld operation. Our first printed version attempted to address the footprint by switching to a rectangular base, but fit tolerances were inconsistent. Several parts required extensive sanding to assemble, and still didn't provide the desired smoothness of motion.

The two rails of the 97-degree arc were originally only joined at the top, leaving the side rails unsupported along most of their length. This made the arc flimsy and prone to bending. To address this, we added geometry to join the rails at the bottom, preventing the rails from getting closer or farther apart. Pressing down on the arc in previous iterations revealed that the arc flexed elastically due to a lack of reinforcement, which compromised both rotational smoothness and angular accuracy. To resolve this, we introduced a tapered support beam beneath the arc. This allowed for more effective load distribution and minimized arc deflection during adjustments.

We uniformly scaled down the device by a factor of two (excluding tolerance-critical joints), making it significantly more compact and easier to position on irregular surfaces. One key redesign involved repositioning the sliding track further from the arc. In earlier versions, the bolt-washer-nut locking mechanism interfered with the syringe clip slider, making it nearly impossible to detach or reattach without partial disassembly. In certain tilt configurations, the track would sit below the base plate level, leading to patient discomfort and potential instability. To resolve this, we increased the distance between the arc and the track, allowing more clearance and ensuring the track would never obstruct the base's contact with the skin. Another functional flaw emerged when we realized the needle length exceeded what we expected when designing. In earlier prototypes, the needle tip would already begin to penetrate the silicone skin before the device was fully positioned. To prevent premature insertion and accommodate longer syringes, we extended the track length and shifted it farther outward from the arc. This allowed the syringe + clip + slider assembly to be loaded as one piece after the angle was locked in. A rectangular hole

was added to the base plate to insert a mini level, providing visual feedback for whether the base was flush with the patient surface. Finally, we introduced a custom-molded silicone base, cured post-print, to conform to the patient's anatomy. The operator can now press around the device's perimeter to ensure full contact, and our physics simulations confirmed that this adjustment technique does not deform the structural components.

Fourth Iteration Design

The fourth iteration consolidated all previous versions into a streamlined, structurally reinforced, and clinically viable prototype. A rectangular cutout was added to accommodate a mini bubble level, providing the operator with clear visual confirmation of whether the device is properly aligned during setup. To improve anatomical conformity, a custom-molded silicone layer was cured beneath the base plate. This silicone

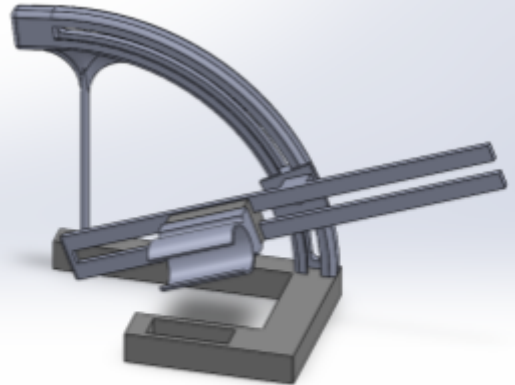


Figure 4 | 3D Model of Assembly. A 3D model from SolidWorks of the fourth version of the needle guide.

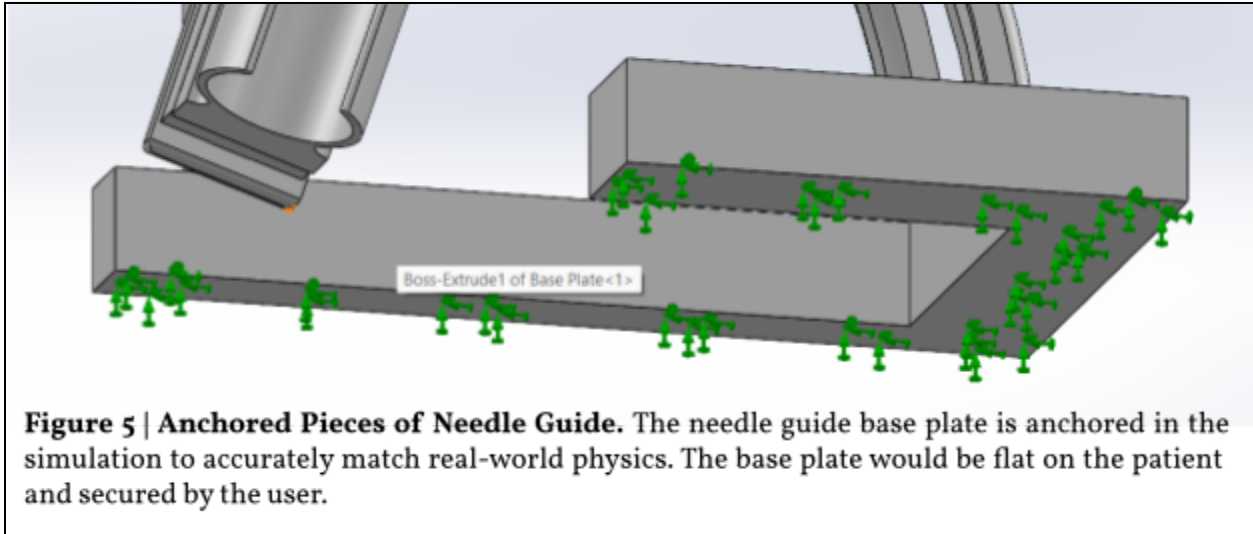
surface deforms locally under operator pressure, enabling full contact with irregular skin surfaces while maintaining device stability. Simulation data confirmed that this compliance does not compromise the mechanical integrity of the device.

The 97-degree arc was reengineered to address prior structural weaknesses. It is now connected at both the top and bottom ends, preventing the rails from separating or collapsing under load. A tapered support beam was added beneath the arc to distribute stress more evenly, eliminate deflection, and maintain accurate angular readings during adjustments. Internal rail profiles were modified to account for imperfections caused by support scaffolds during 3D printing, ensuring smooth and consistent motion along the arc.

The rotating track was extended to approximately twice the radius of the arc. This increased travel distance enables the syringe clip and slider assembly to remain fully outside the base plate until after the angle adjustments are locked in, thereby resolving the premature insertion issue that occurred in earlier versions. The locking mechanism—a bolt, washer, and nut—no longer interferes with the syringe clip thanks to the revised placement and orientation of the track. The clip and slider can now be attached and removed independently, which greatly improves usability and assembly speed.

Together, these changes reflect a shift away from overengineered or redundant systems toward a lean, purpose-built guide. Each design feature directly supports the clinical requirements of stability, precision, and ease of use in minimally invasive procedures.

b. Physics Simulations



The device is designed to sit level on the patient, allowing us to fix the bottom of the base plate for physics simulations. Our device is expected to be exposed to three main forces:

- I. The top of the arc is subjected to the force from the operator's hand, which secures the device and prevents tipping over when adjusting the syringe angle of entry. We assume that only the weight of the hand is exerted downwards and no extra force is applied. The average weight of the human hand is 400g, so the force of gravity exerted on the arc is:

$$0.400\text{kg} \times 9.8 \text{ m/s}^2 = 3.92\text{N}$$

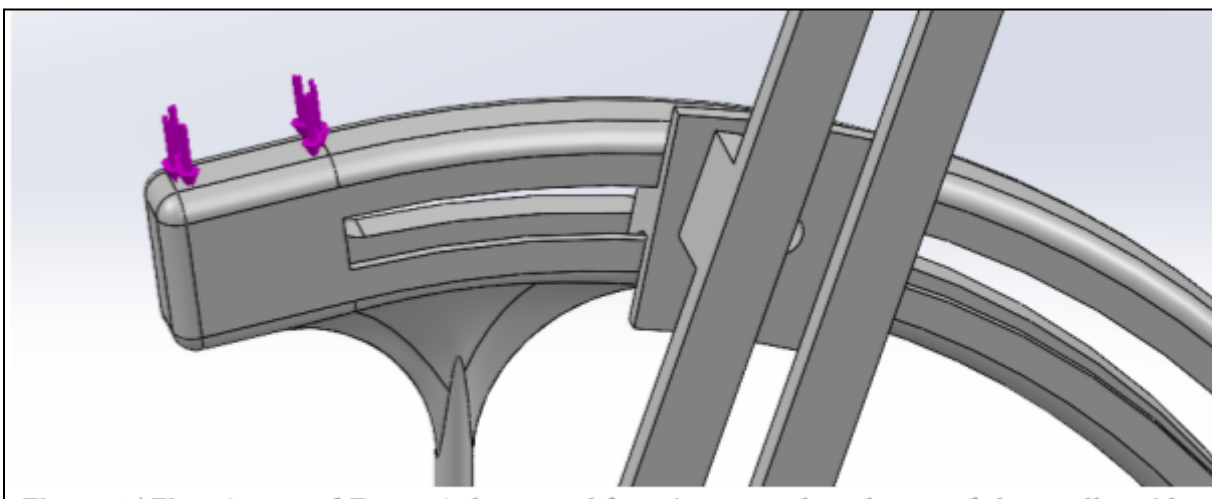


Figure 6 | First Assumed Force. A downward force is expected on the top of the needle guide from the user. The force secures the needle guide in place on the patient.

II. The attached syringe would cause a downward force on the track, pulling down on the arc asymmetrically. The weight of the syringe in this case was overapproximated for safety as 50g, the force exerted is calculated to be: $0.050\text{kg} \times 9.8 \text{ m/s}^2 = 0.49\text{N}$

III. When the operator adjusts the track angle along the arc, the hand would press against the plate; we assumed the force would be less than the weight of the hand, so we approximate it as 1N

Figure 8 | Force Applied to Connecting Rail. The force applied to the connecting rail is depicted using the purple arrows. The force is generated by the operator adjusting the rail along the track.

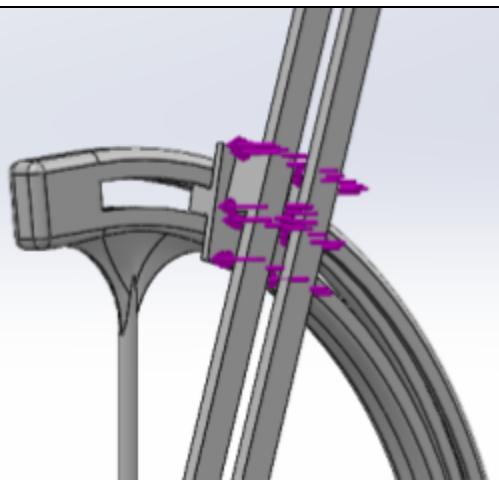
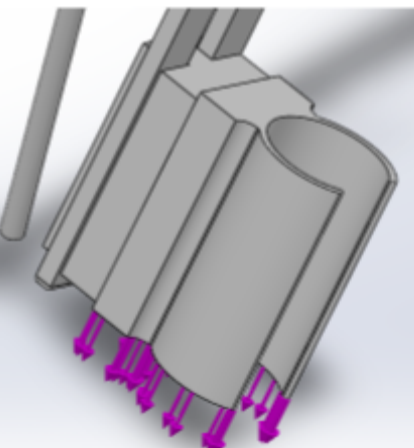
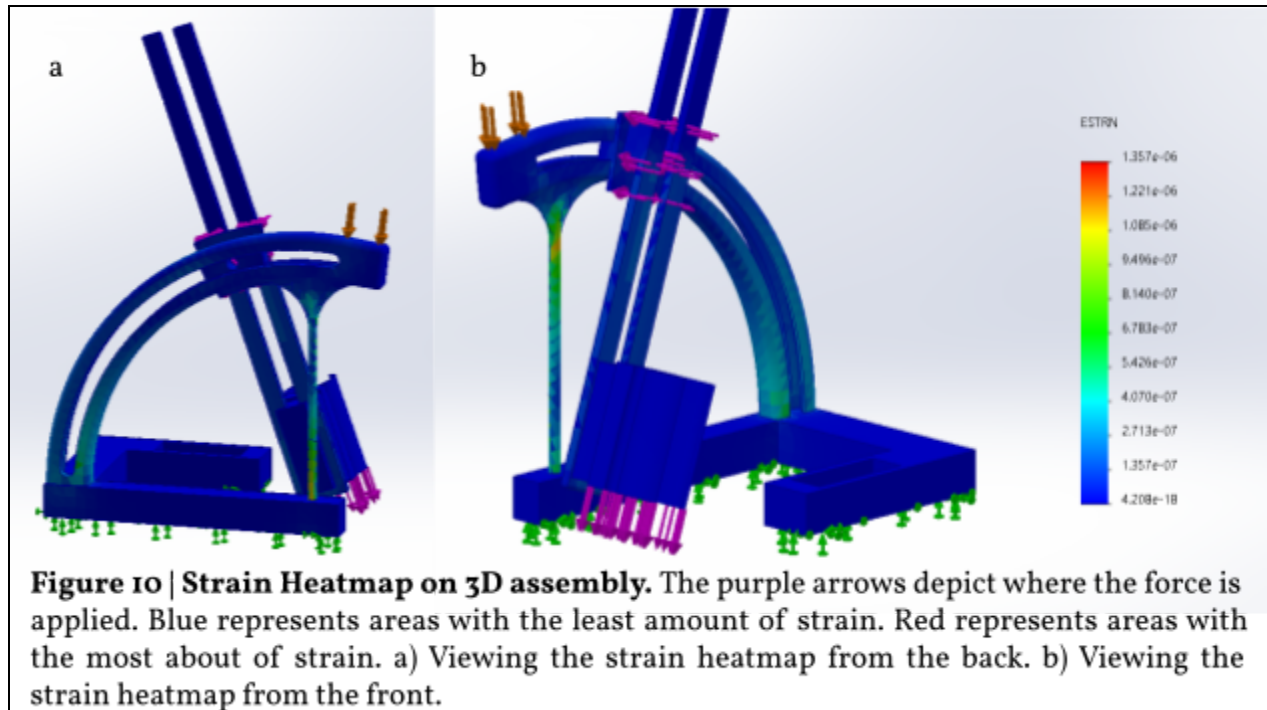


Figure 7 | Force Applied on Needle Clip. The downward force from the operator is depicted by the purple arrows. The force is generated as the operator adjusts the position of the syringe using a railing system.



c. Results

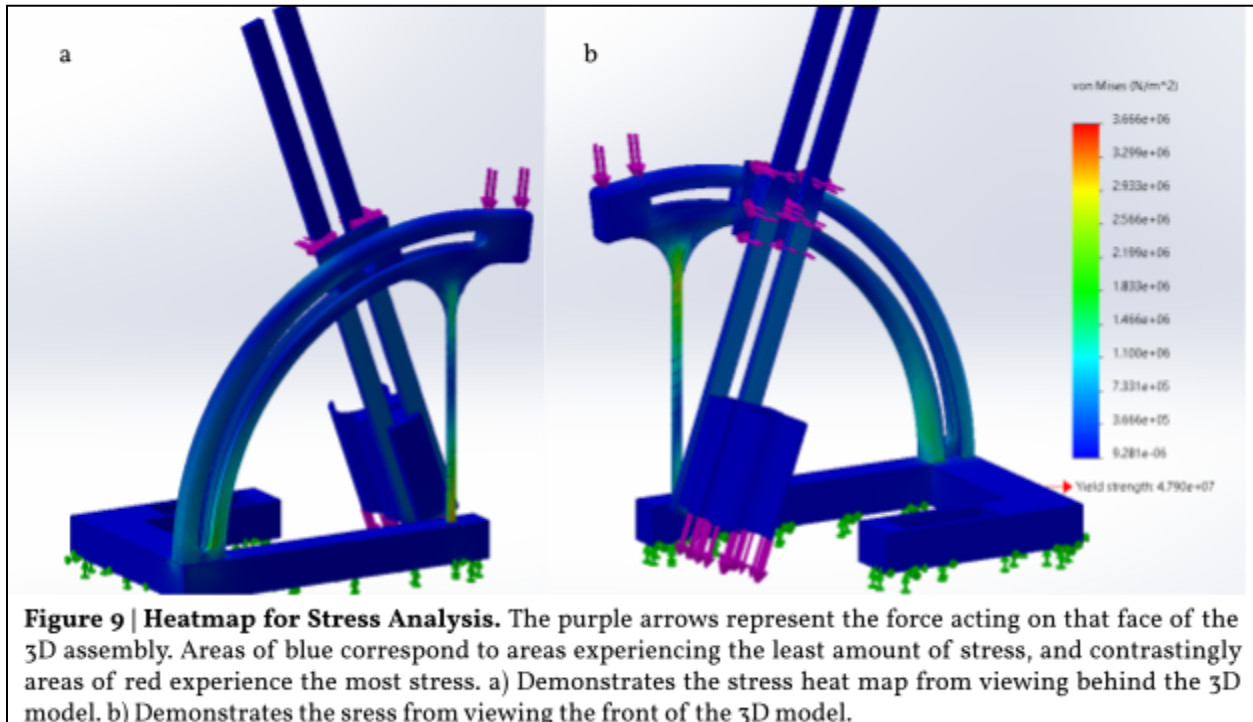
To better visualize the effects of loading on the device, SolidWorks Simulation was used to generate animations of stress, strain, and displacement. These animations simulate the gradual application of force from 0% to 100% of the defined load, interpolating the model's deformation and the development of internal stresses: [Physics Simulation Animations](#)

Stress Heatmap

Stress (denoted σ) describes the internal resistance of a material to deformation when a force is applied. It is usually approximated as the force divided by the area under load:

$$\sigma = \frac{F}{A}$$

Most of the arc and support structures remain in the blue to green stress regions, indicating low stress throughout the device. Only small concentrations of stress appear near screw holes and interfaces—expected zones due to localized constraints and loads. PTEG (Polyethylene Terephthalate Glycol) has a yield strength (Maximum stress before permanent deformation) of approximately 47.95 MPa, as shown on the legend scale. The maximum von Mises stress observed is well below 5 MPa, indicating a conservative safety factor greater than 10. This predicts that the device will remain in the elastic deformation range under all anticipated operating conditions.

Strain Heatmap

Strain (denoted ε) is a dimensionless quantity that describes how much an object deforms relative to its original shape. It is defined as the ratio of the change in length divided by the original length:

$$\varepsilon = \frac{\Delta L}{L_0}$$

The maximum strain observed in the model is approximately 1.35×10^{-6} , as shown in the red areas of the heatmap. This is an extremely low strain value, suggesting that the deformation of the device under expected operational loads is negligible. These strain values indicate the device operates well within the elastic region of the PTEG material. Even under the combined weight of the operator's hand and syringe (~4.4 N total), the device is not expected to undergo permanent deformation. Low overall strain ensures the angular accuracy of the arc remains intact during use, which is critical for maintaining precise needle alignment. This validates the mechanical rigidity and usability of the final design in a clinical context.

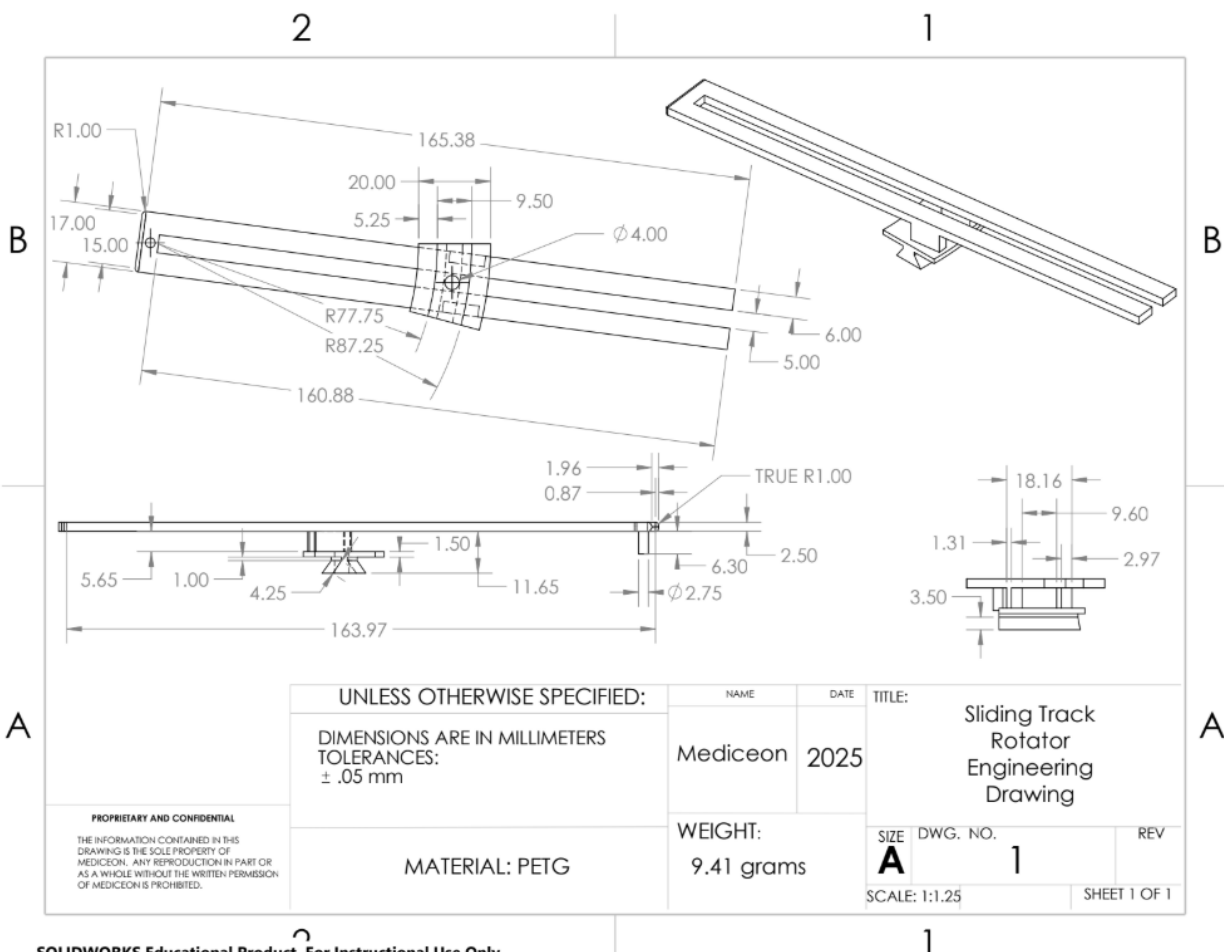
Motion Study

Mediceon Guided syringe motions were to address Dr. Pham's design criteria. The three main components that needed to be incorporated were depth, slice, and angle. Each main component, therefore, has an associated motion. The first movement occurs between the Rotator track and the Sliding Rotator track. With the Rotator track being fixed, the Sliding rotator track moves along the path of the Rotator track. What would induce this motion would be the hand of a surgeon, and what keeps the Sliding rotator track on this path is a rail system that physically

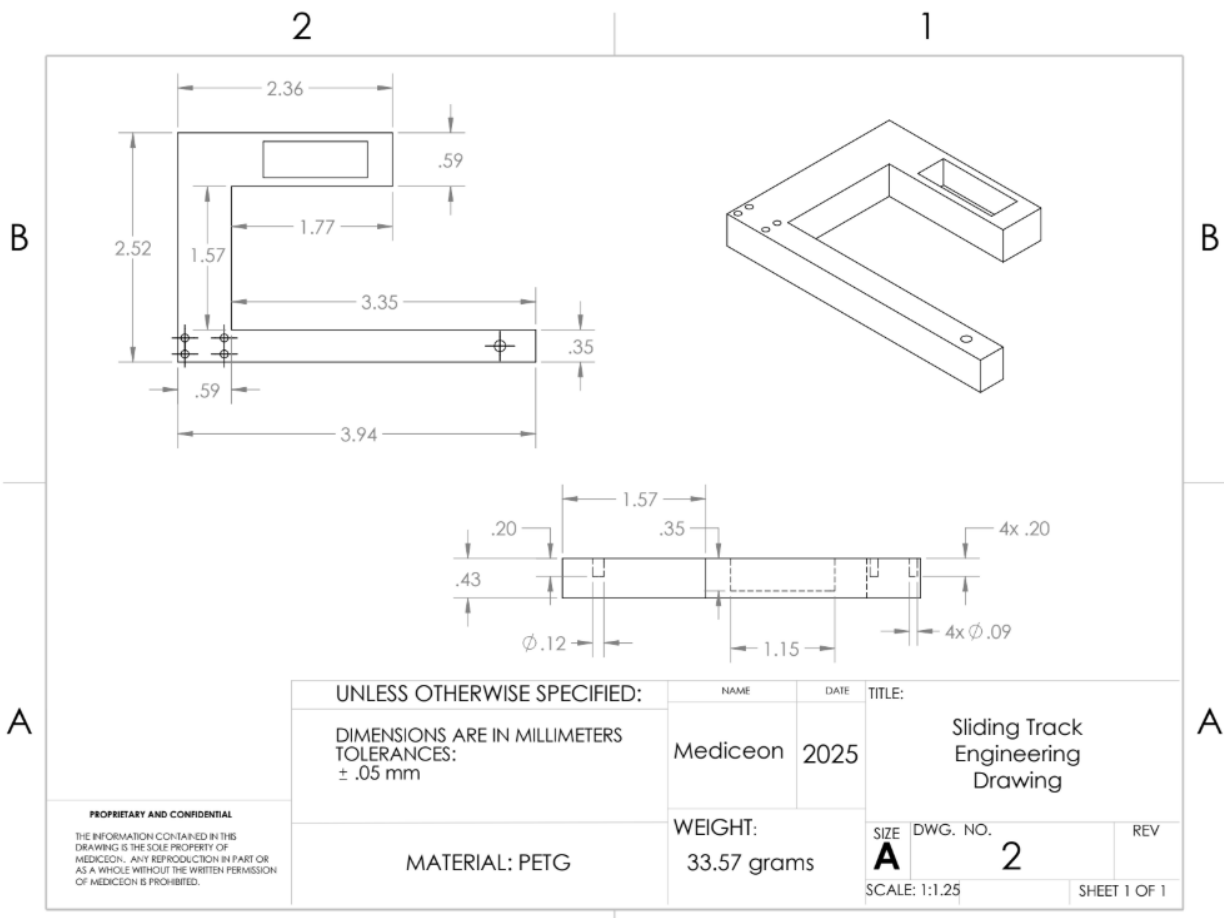
restricts movement. This movement addresses the angle as the Rotator track is modeled after a protractor. The angle expressed is between 7.5-90 degrees, which can be thought of as the first quadrant in math terms. The restriction to the first quadrant and not all the quadrants is addressed by the other motions that allow us to address any degree necessary for surgery. The second movement is between the slider attachment and the sliding rotator track. With the Sliding rotator track being fixed relative to the slider attachment. The slider attachment moves linearly along the length of the Sliding rotator track. The surgeon induces this motion; what keeps the Slider attachment on the Sliding rotator track is another rail system. The movement would follow the same movement of an insertion of a needle, and as such, does not impede the predetermined length of the needle. The third movement involves relocating the Base plate along with all other attached components. This movement is from the surgeon picking up the device to reorienting to the correct location. The freedom to place the device anywhere on the body allows for quick adjustments. This movement is also important to address by adjusting the device's location to match the MRI-produced slice, ensuring that the surgeon inserts it along the correct path.

[All Three Motion Studies](#)

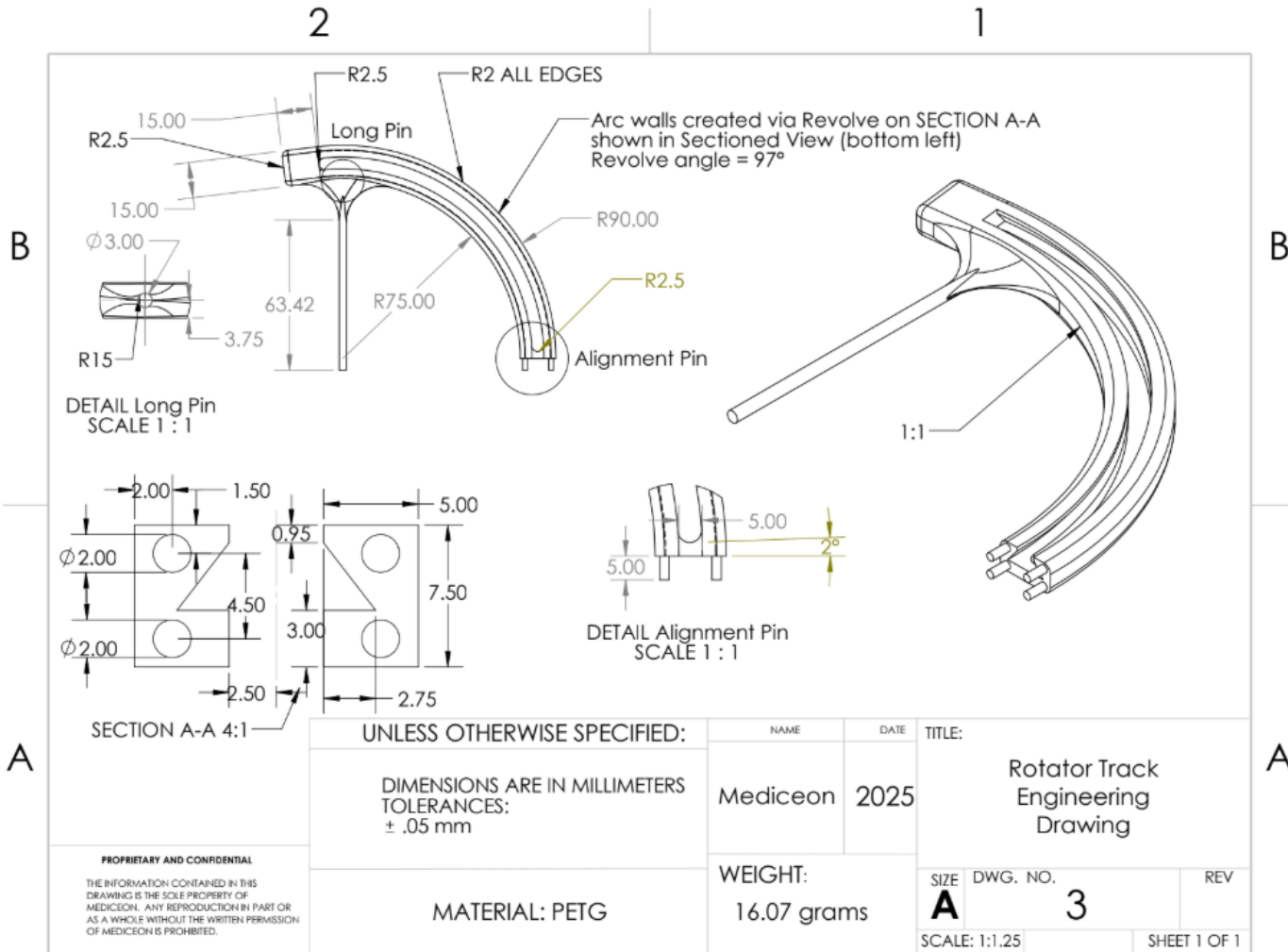
d. Engineering Drawings



[Sliding Track Build Tutorial](#)

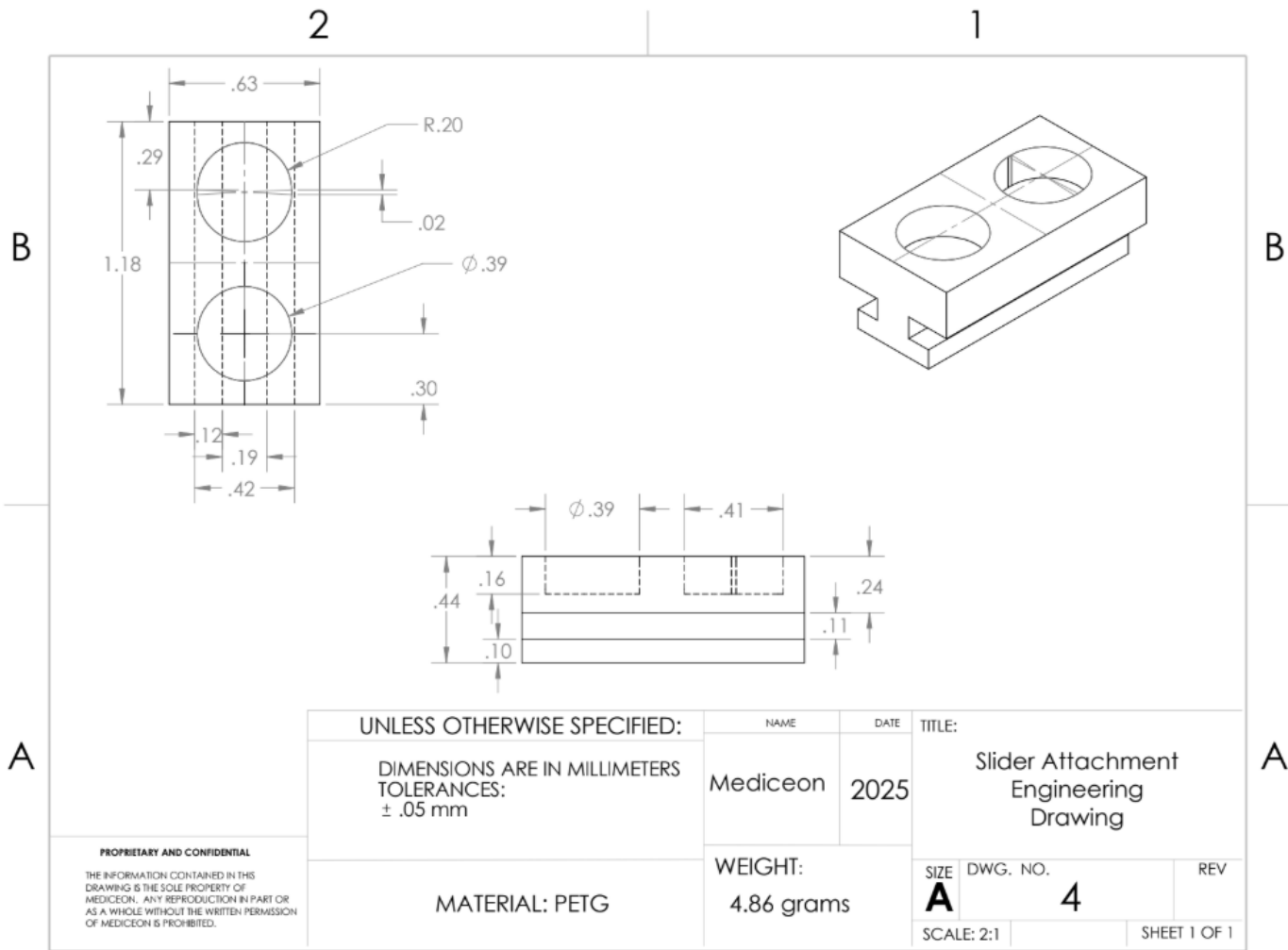


Base Plate Build Tutorial

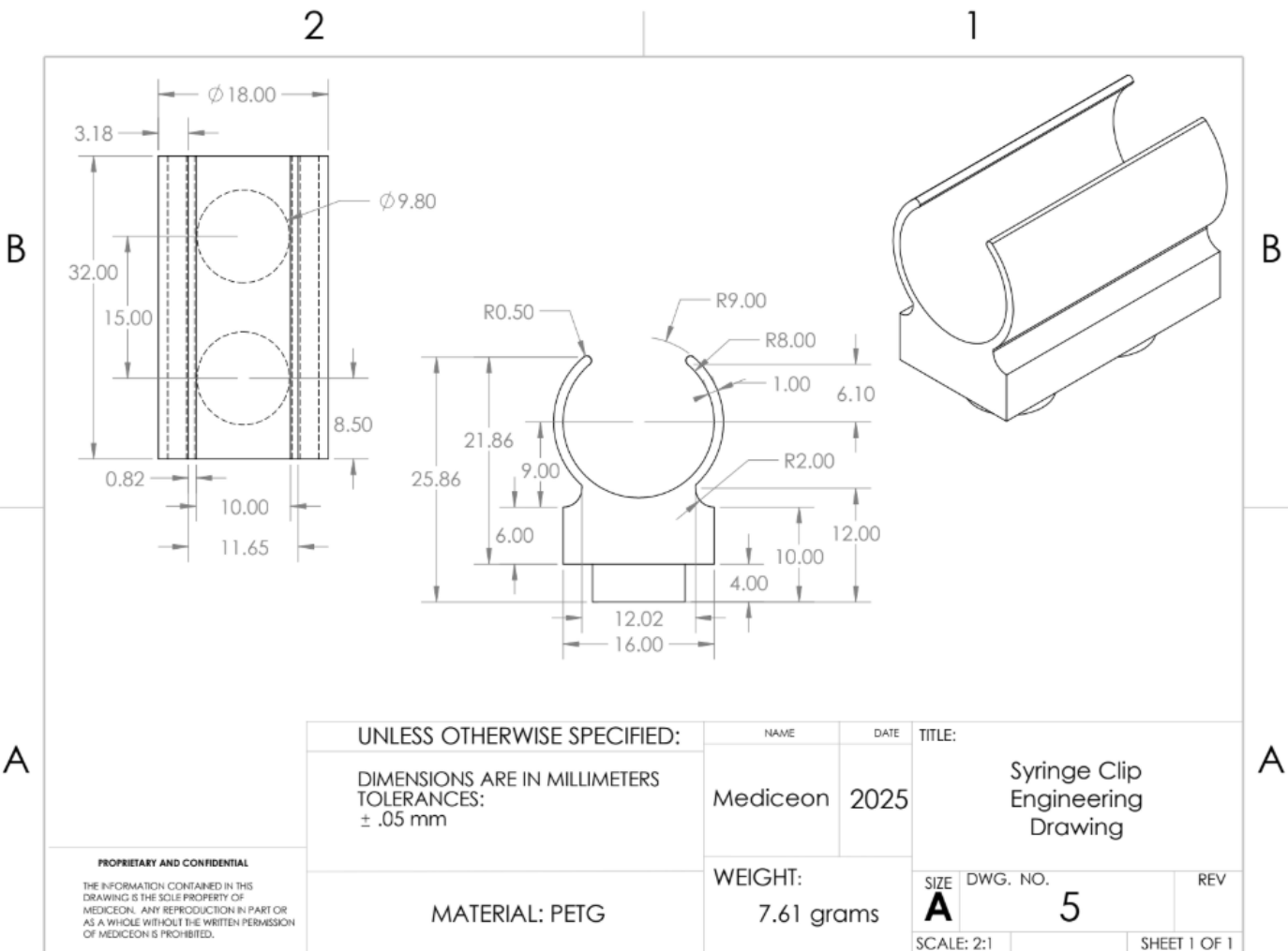


SOLIDWORKS Educational Product. For Instructional Use Only.

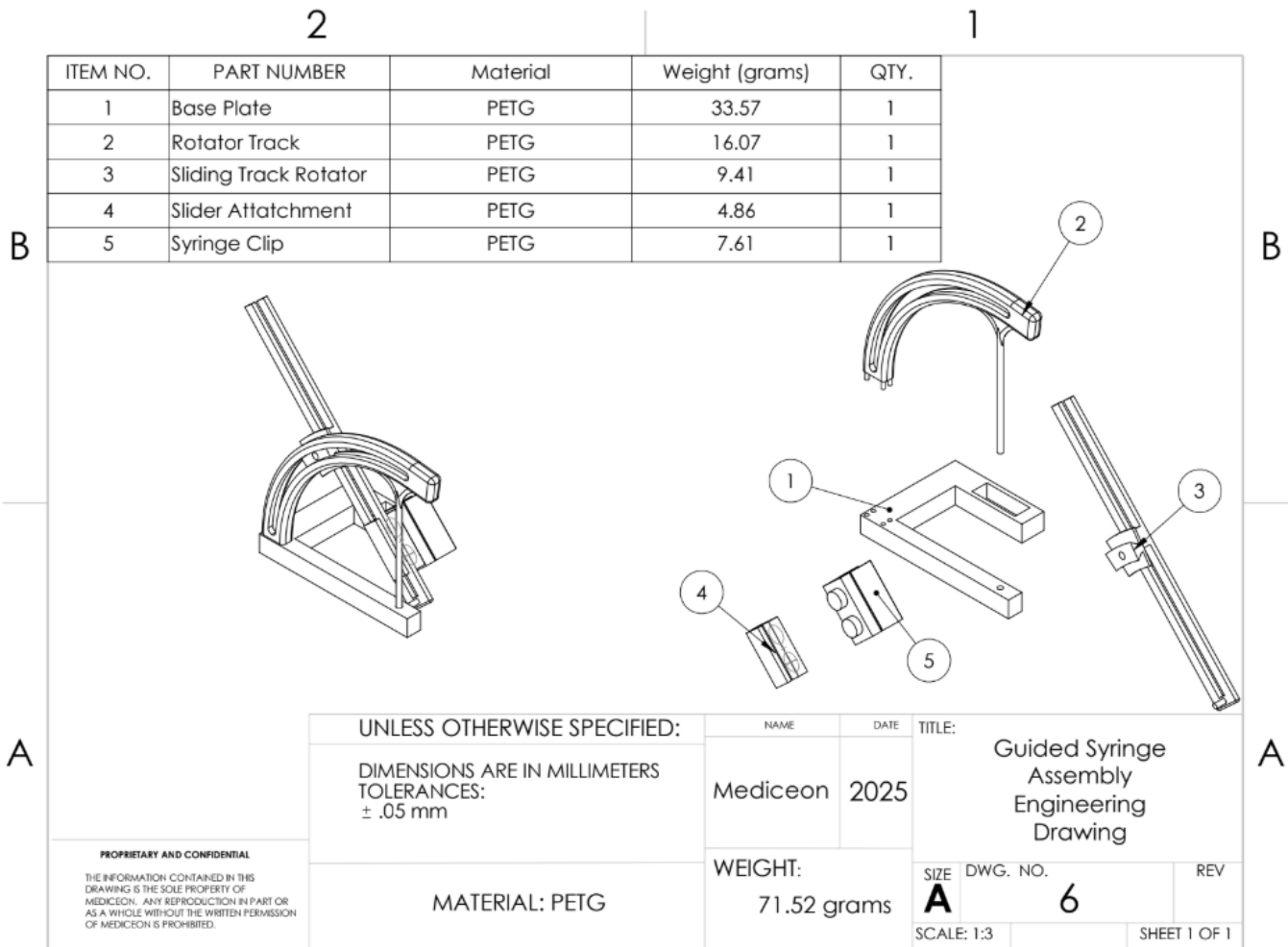
Rotator Track Build Tutorial



Slider Attachment Build Tutorial



[Syringe Clip Build Tutorial](#)



[Assembly Tutorial](#)

References

“Product Classification.” Fda.gov, 2025,

www.accessdata.fda.gov/scripts/cdrh/cfdocs/cfpdc/classification.cfm?id=GDF.

Contains Nonbinding Recommendations Draft -Not for Implementation Select Updates for Biocompatibility of Certain Devices in Contact with Intact Skin Draft Guidance for Industry and Food and Drug Administration Staff DRAFT GUIDANCE. 8 Sept. 2023.

<https://www.accessdata.fda.gov/scripts/cdrh/cfdocs/cfpdc/classification.cfm?id=GDF>.

Hiraki, T., Matsui, Y., Sakurai, J., Tomita, K., Uka, M., Kajita, S., Umakoshi, N., Iguchi, T., Yoshida, M., Sakamoto, K., Matsuno, T., & Kamegawa, T. (2025). Comparison of robotic versus manual needle insertion for CT-guided intervention: Prospective randomized trial. Radiology Advances, 2(2), umaf010.

<https://doi.org/10.1093/radadv/umaf010>

VanSonnenberg, E. “Triangulation Method for Percutaneous Needle Guidance: The Angled Approach to Upper Abdominal Masses.” American Journal of Roentgenology, 23 Nov. 2012,
ajronline.org/doi/10.2214/ajr.137.4.757.

Siemens Healthineers. (n.d.). CT-guided interventions. Retrieved June 9, 2025, from
<https://www.siemens-healthineers.com/fi/computed-tomography/ct-clinical-fields/ct-guided-interventions>

Thomas, X, et al. 7. Silicones in Medical Applications.

<https://www.pentasil.eu/images/Chapter%2017%20Silicones%20in%20Medical%20Applications.pdf>

Prasetyono, Theddeus Octavianus Hari, and Prasasta Adhistana. "Laboratory Study on Injection Force Measurement on Syringe and Needle Combinations." *The Malaysian Journal of Medical Sciences: MJMS*, vol. 26, no. 2 (2019): 66-76. doi:10.21315/mjms2019.26.2.8

Ling, Xuanzhe & Jing, Xishuang & Zhang, Chengyang & Chen, Siyu. (2020). Polyether Ether Ketone (PEEK) Properties and Its Application Status. *IOP Conference Series: Earth and Environmental Science*. 453. 012080. 10.1088/1755-1315/453/1/012080.